Performance of a test embankment constructed on an organic clayey silt deposit

R. Kerry Rowe, C.T. Gnanendran, A.J. Valsangkar, and A.O. Landva

Abstract: The instrumentation, construction, and field performance of a full-scale test embankment constructed on a soft compressible organic clayey silt is described. The construction sequence, the observed vertical and horizontal displacements, and the pore pressure response are presented. The embankment behaved elastically up to a thickness of about 3.65 m. The settlement and heave responses suggested that the embankment approached failure at a thickness of about 6.1 m and a corresponding net height of 5.4 m. The failure was gradual and of a viscoplastic type, and no classical-type abrupt failure was encountered during the construction of this embankment. The height to which the embankment could be constructed was lower than the 7–11.4 m range expected from conventional two-dimensional (2D) limit equilibrium analysis based on vane strength data. This, coupled with the pore pressure response, suggests that a combination of progressive failure and the influence of the adjacent reinforced section constructed to failure may have been significant factors affecting the performance of this embankment. Thus, the data reported in this paper can be used as a test case for developing three- dimensional (3D) analysis methods wherein the constitutive model can be truly tested for 3D conditions involving the interaction between embankment sections that are constructed under different conditions.

Key words: embankment, field behaviour, stability, deformations, pore pressures.

Résumé :On décrit l'instrumentation, la construction et le comportement sur le terrain d'un remblai d'essai construit sur un silt argileux organique mou et compressible. Cet article présente le cheminement de la construction, les déplacements verticaux et horizontaux observés, de même que la réponse de la pression interstitielle. Le remblai s'est comporté en mode élastique jusqu'à une épaisseur d'environ 3,65 m. Les comportements en tassement et en soulèvement ont indiqué que le remblai s'approchait de la rupture à une épaisseur d'environ 6,1 m, soit une hauteur nette de 5,4 m. La rupture a été graduelle et de type viscoplastique; il ne s'est pas produit de rupture abrupte de type classique durant la construction de ce remblai. La hauteur à laquelle le remblai aurait pu être construit a été plus faible que la plage de 7 à 11,4 m donnée par l'analyse d'équilibre limite bidimensionnelle conventionnelle utilisant les données de résistance au scissomètre. Cette observation combinée avec la réaction de la pression interstitielle indique qu'une combinaison de rupture progressive et de l'influence de la section adjacente armée construite jusqu'à la rupture peuvent avoir été des facteurs significatifs qui ont affecté le comportement de ce remblai. Ainsi, les données présentées dans cet article peuvent être utilisées comme un cas d'essai typique pour développer des méthodes d'analyse tridimensionnelle dans lesquelles le modèle de comportement peut vraiment être testé pour des conditions 3D impliquant l'interaction entre des sections de remblais qui sont construites dans des conditions différentes.

Mots clés : remblai, comportement en nature, stabilité, déformation, pressions interstitielles.

[Traduit par la Rédaction]

Introduction

Soft compressible organic clayey silt deposits are found in many parts of Canada, including Eastern New Brunswick where several road construction projects have recently been completed. One such project is the widening of the two-lane Trans-Canada highway into a divided dual carriage highway between Moncton in New Brunswick and Amherst in Nova Scotia. Several sections of this road involved the construction of 2–4 m high embankments on soft compressible organic clayey silt soils. Special measures such as preloading, stage construction, and slope and height restrictions have been employed to satisfy stability requirements. A test embankment was constructed prior to roadway construction to gain better insight into the behaviour of these soft soils.

The performance of embankments constructed on soft clays has been studied by many researchers (e.g., Hoeg et al. 1969; D'Appolonia et al. 1971; Leroueil et al. 1978*a*, 1978*b*; Tavenas and Leroueil 1980; Parry and Wroth 1981; Ortigao et al. 1983; Indraratna et al. 1992; Loganathan et al. 1993; Crawford et al. 1995; Fernando 1996; Asaoka et al. 1998; Hussein and McGown 1998; Hinchberger and Rowe 1998; and many others). Full scale instrumented test embankments

Received October 19, 2000. Accepted May 17, 2001. Published on the NRC Research Press Web site at http://cgj.nrc.ca on January 10, 2002.

R.K. Rowe.[1] Department of Civil Engineering, Queen's University, Kingston, ON K7L 3N6, Canada.
C.T. Gnanendran. School of Civil Engineering, University College, University of New South Wales, Canberra, ACT 2600, Australia.
A.J. Valsangkar and A.O. Landva. Department of Civil Engineering, University of New Brunswick, Fredericton, NB E3B 5A3, Canada.

[1]Corresponding author (e-mail: kerry@civil.queensu.ca).

 DOI: 10.1139/cgj-38-6-1283

and the measurements obtained from the previous studies provide valuable data for understanding embankment behaviour, investigating the validity of theories and assumptions used for analysis and design, and the development of improved design methods (e.g., see Leroueil and Rowe 2000).

This paper reports results obtained from an instrumented test embankment constructed between Sackville and Aulac in the province of New Brunswick, Canada. The objective of this test embankment was to provide a case record of deformation and progressive failure for geotextile reinforced and unreinforced embankment sections constructed on a soft compressible organic clayey silt. The behaviour of the geotextile reinforced section was reported by Rowe et al. (1995). The observed behaviour of the unreinforced section of the test embankment is described in this paper. Pore pressure responses, settlement, heave, lateral displacements, and the failure of the unreinforced embankment are discussed.

Soil profile and brief description of test embankment

A plan view of the test embankment configuration is shown in Fig. 1. The test site is situated in an area of intertidal salt marsh deposit (Rampton and Paradis 1981) and the profile of the foundation soil established from the site investigation is shown in Fig. 2. A typical borehole log of the foundation soil and the results of index tests on undisturbed samples retrieved by NRC (National Research Council of Canada), University of New Brunswick static cone penetration tests (denoted as "UNB cone tests" in Fig. 1), and field vane tests are shown in this figure. Details concerning the site conditions and the design of the test embankment configuration have been given by Rowe et al. (1995), and additional data relating to the rate dependent characteristics of the soil have been given by Rowe and Hinchberger (1998).

The liquidity index of the soil exceeded 1 at depths ranging from 1 to 6 m. The sensitivity of the clayey silt was in the range of 2.4–5.6, with higher values near the ground surface (ranging between 3.2 and 5.6 for depths less than 4 m). The initial site investigation consisting of UNB cone tests at two locations (i.e., the cone data presented in Fig. 2) indicated that there was a root mat underlain by organic clayey silt – silty clay whose strength increased with depth. Since the objective of this test embankment was to examine the response of the organic clayey silt – silty clay below the root mat, 1–1.2 m deep vertical cuts on an approximately 1.3–1.8 m square grid were made in the root mat to minimize its effect on the overall response.

The test embankment consisted of a 25 m long unreinforced section and a 25 m long geotextile reinforced section along the east–west axis. The two sections were connected by a reinforced transition; the reinforcement extending up to approximately 15 m east of the line defining cross-section A-A in Fig. 1. The embankment configuration was designed in such a way that failure would take place only on the northern side. This was a critical design constraint because of the very close proximity of the NBTel fibre optic cable just south of the embankment. Berms were provided in the east, west, and southern sides as detailed in Fig. 1 (see also Fig. 3).

Both the NRC cone data and vane data indicated that the soil strength varied at shallow depths (< 4 m) over the site; being 20–30% higher beneath what was selected to be the unreinforced section (see Fig. 2) than beneath the reinforced section. Based on this information, it was considered best to arrange the sections so that the stronger soil was beneath the unreinforced section, thereby minimizing the difference in fill thickness required to fail the two sections. Two-dimensional limit equilibrium analyses performed on the basis of the range in vane strength values indicated that the failure height of the unreinforced embankment would range between 7 and 11.4 m and that of the reinforced embankment would range between 6.6 and 11.1 m. The failure heights were calculated to be 9.2 and 8.8 m, respectively, for the unreinforced and reinforced embankments based on an average vane strength profile beneath each section (see Fig. 2 for vane strength profiles). The geometry of the test embankment was such that true plane strain conditions could not be achieved for either the reinforced or the unreinforced sections, although the reinforced case approached plane strain. The primary focus of the study was on the reinforced section that was loaded to failure in a way that best approximated plane strain conditions. Having done so, the loading of the unreinforced section to failure provided an opportunity to collect data that the writers considered would be useful for testing future 3D numerical models.

Instrumentation

The mid portion of the unreinforced section was instrumented with piezometers, settlement plates, augers, heave plates, inclinometer casings, and a total pressure cell as shown in Figs. 1 and 3. These instruments were installed in June 1989 (i.e., approximately 3 months before construction).

To monitor the development of excess pore pressures in the foundation subsoil, a total of ten pneumatic (PETUR^{TM} P-102 wellpoint type) piezometers were installed at various depths as shown in Fig. 3. Four heave plates, four settlement plates, and three augers at different depths were installed on the main part (i.e., northern side) of the unreinforced embankment to monitor the movement of the specific points on the ground surface and the foundation soil. Another set of three augers at different depths, two settlement plates, and three heave plates were installed on the berm (i.e., southern) side of the embankment (see Figs. 1 and 3). Lateral displacement of the foundation subsoil was monitored with three vertical inclinometers that were installed close to the toe of the embankment (see Figs. 1 and 3). Inclinometer casings were installed up to a depth of about 10 m, where a stratum of stiff clayey silt was encountered. A pneumatic total pressure cell was installed close to the centerline of the unreinforced section to measure the pressure imposed by the fill on the foundation subsoil.

Embankment construction

The instrumentation was monitored prior to construction, until its initial performance was considered to be satisfactory and zero readings were defined. Initially, a 0.5 m thick gravel access road was formed, avoiding the instrumented zones. A 0.3 m thick blanket of the same gravel was placed

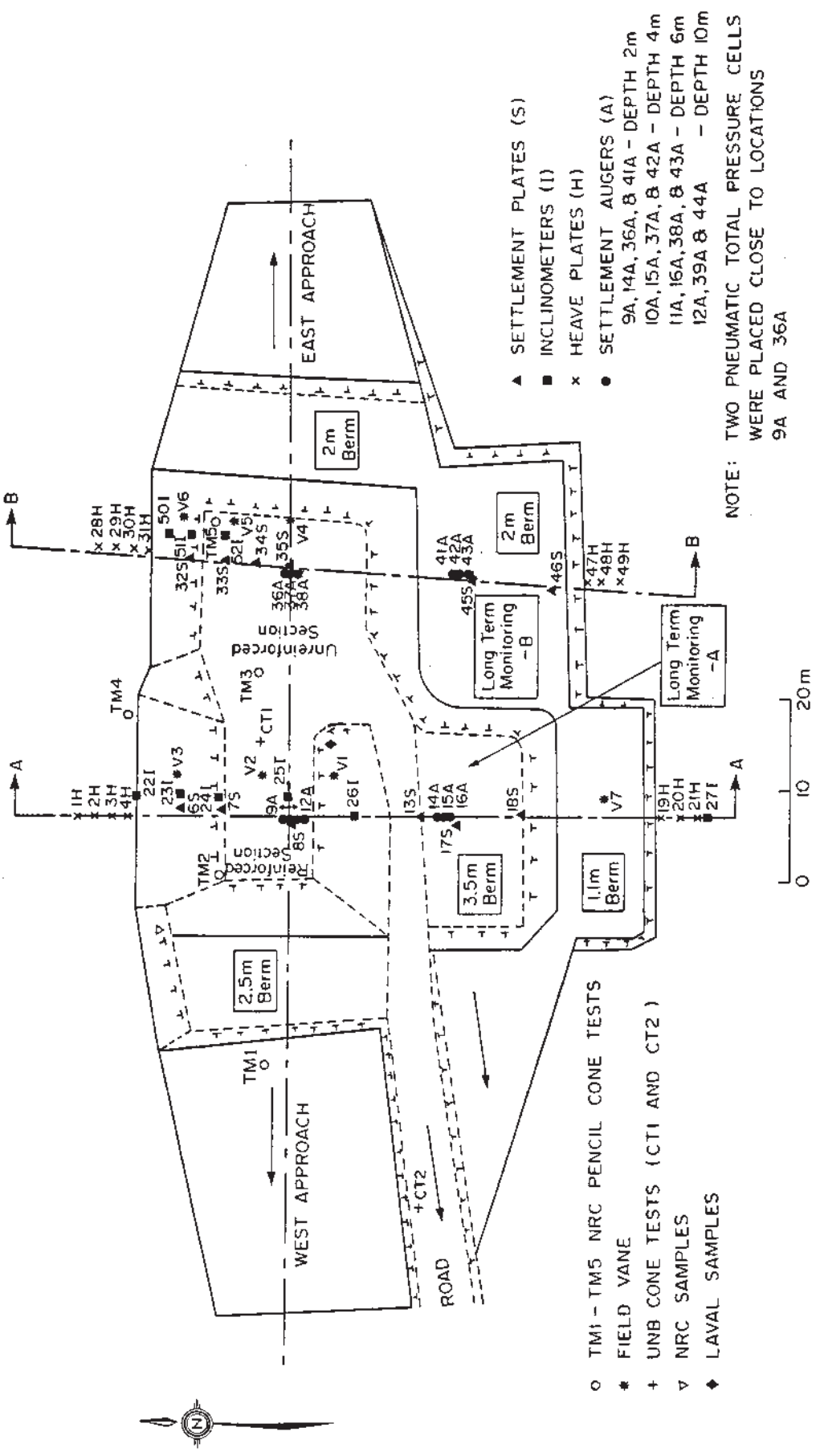

Fig. 1. A plan view of the embankment configuration and instrumentation layout.

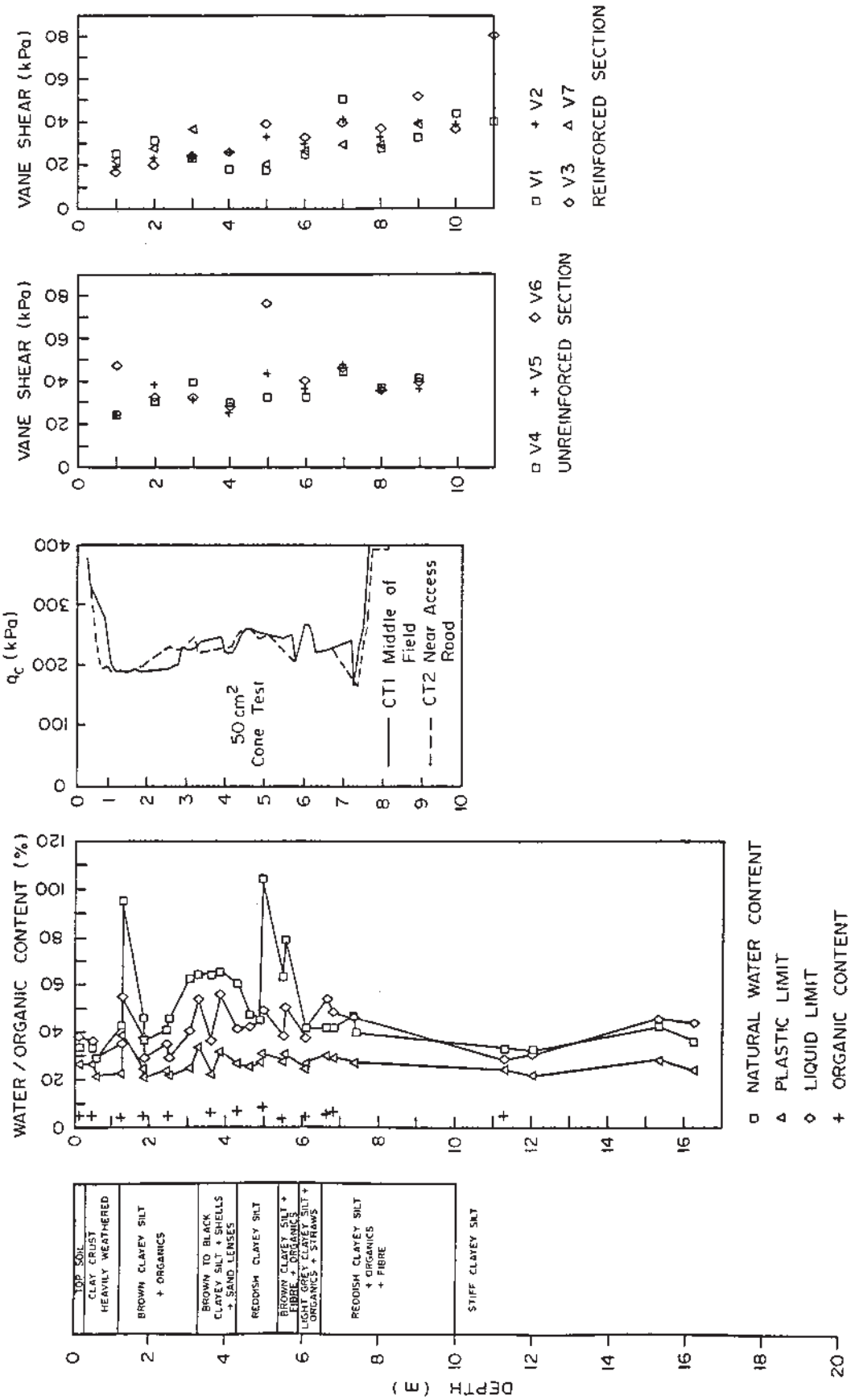

Fig. 2. Foundation soil profile.

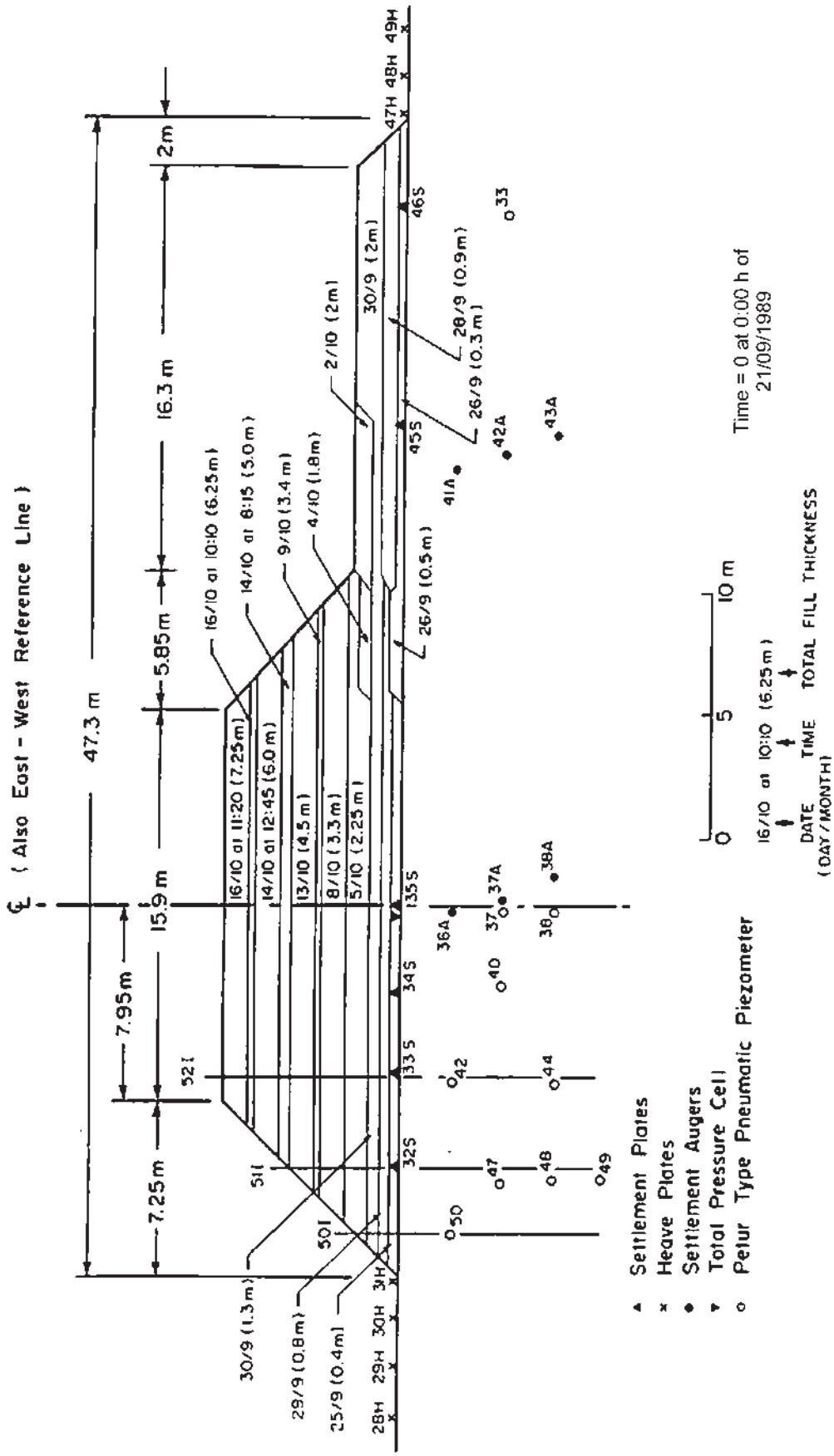

Fig. 3. Layout of instrumentation and sequence of construction.

Fig. 4. Variation of embankment thickness and total pressure cell reading with time.

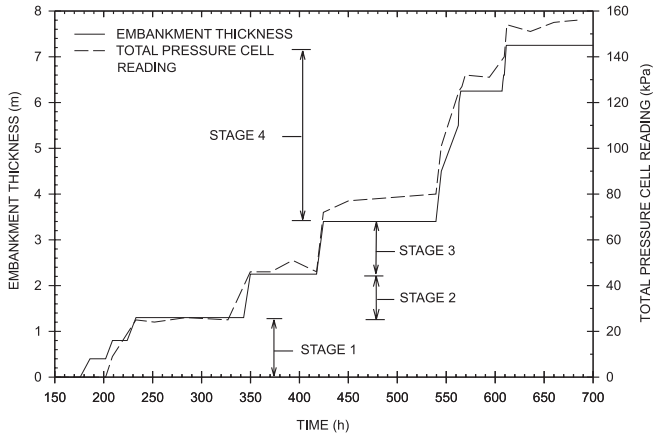

Fig. 5. Shear strength envelope of embankment fill.

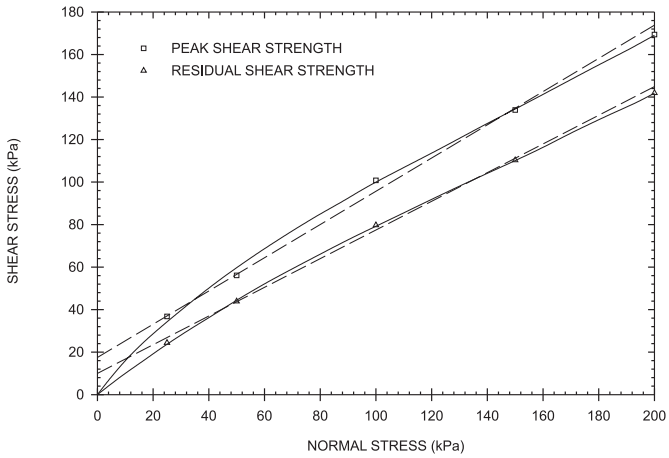

on the waterlogged areas found on the southern side of the section. A locally available gravelly silty sand containing some clay was used as the fill material. Utmost care was taken not to allow passage of the trucks directly over the instruments or the piezometer leads. A medium weight bulldozer was used for the spreading and compaction processes.

Construction of the embankment was performed in four stages (Fig. 3). During the first, second, and third stages, the thickness of fill in the northern side of the embankment was increased to 1.3, 2.25, and 3.4 m, respectively. In the last stage of construction, it was rapidly built to failure over a 3-day period (see Figs. 3 and 4).

The mean fill unit weight, as determined by in situ tests, averaged 19.6 kN/m^3, with a standard deviation of 1.0 kN/m^3. During construction of the embankment as well as the berms, the fill was found to stand at a slope of about 45°. Direct shear tests on saturated bulk samples of fill with 25–200 kPa normal stress indicated the following linearized strength parameters (see Fig. 5):

Parameter	c' (kPa)	ϕ' (°)
Peak strength	17.5	38
Residual strength	10	34

where c' is the cohesion and ϕ' is the internal angle of friction.

The piezometers and the position monitoring devices (i.e., settlement plates, heave plates, and augers) were monitored at least twice a day when construction was in progress, but more frequently at later stages of construction when there was evidence of rapid movement. A full set of readings was taken after placement of each layer of fill shown in Fig. 3.

Results and performance of instrumentation

Embankment thickness and total pressure

Fill thicknesses were monitored by observing the position of the surface of fill against the fill thickness scale markings made on the settlement plate extension pipes. The variation of thickness of the main part (i.e., northern side) of the unreinforced section of the embankment (hereafter called the embankment thickness) with time is shown in Fig. 4. The total pressure cell readings were found to be reasonably consistent and in close agreement with the pressures calculated based on thickness and unit weight of the fill, as shown in Fig. 4.

Pore pressures

The variations of excess pore pressure with time and embankment thickness for the different pneumatic piezometers installed in the foundation soil beneath the embankment are shown in Figs. 6, 7, and 8. For convenience of presentation, the data are presented in terms of the time elapsed (in hours) from a reference time of 0:00 h on the day embankment construction commenced. For ease of comparison with the construction sequence, the variation of fill thickness with time is superimposed on the excess pore pressure versus time figures. Although pore pressures increased in direct response to the addition of fill, they also typically continued to rise between different stages. The unreinforced embankment was constructed quite rapidly above 3.4 m thickness and it failed before it reached a thickness of 6.25 m, as will be discussed later in this paper.

Despite some difference in the absolute magnitude of the excess pore pressure, Fig. 6 shows that the response of piezometers 37, 38, and 40 (which were all located near the embankment centerline) was very similar. The excess pore pressure in piezometer 37 (placed closer to the centerline) was always a little greater than that of piezometer 40 even though these two piezometers were installed at the same depth. This difference is attributed to the shorter lateral drainage path for piezometer 40 than that for piezometer 37. Typically, piezometer 38 (placed 2 m below piezometer 37) also showed slightly larger excess pore pressure than piezometer 37. Dissipation of excess pore pressure during the early stages of construction has previously been reported by Leroueil et al. (1978*a*) and Ortigao et al. (1983), among others. Leroueil et al. (1978*b*) analyzed this typical behaviour and attributed the dissipation to the initially overconsolidated state of the foundation soil at early stages and its change to a normally consolidated state at later stages of construction. A similar type of behaviour is evident during the early stages of construction for the Sackville embankment reported here.

Fig. 6. Excess pore pressure variation with time for piezometers 37, 38, and 40.

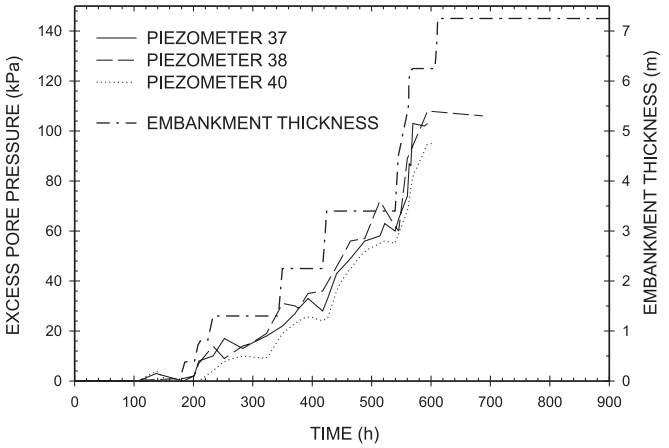

Fig. 7. Excess pore pressure variation with time for piezometers 42 and 44.

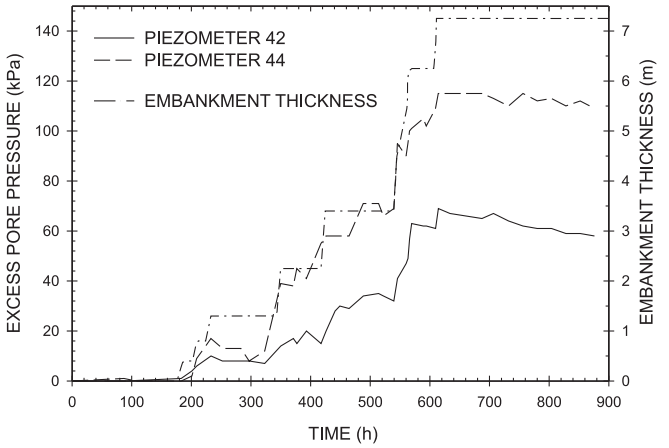

Very rapid build-up of pore pressure was evident in all of the piezometers as the fill was raised from 3.4 to 6.25 m and particularly after the embankment reached a thickness of 5.5 m (i.e., after 560 h). Unfortunately, piezometers 37 and 40 ceased to function after the embankment was constructed to 6.25 m thickness (i.e., after about 600 h); this failure of the piezometers is considered to have been the result of the large deformations that occurred around this time.

Piezometer 44, installed at 6 m depth near the shoulder of the embankment, indicated excess pore pressures comparable to those indicated by piezometers 37, 38, and 40 located near the centerline. However, piezometer 42 installed at 2 m depth (i.e., 4 m vertically above piezometer 44) generally indicated lower excess pore pressures compared to the other four piezometers being discussed (see Figs. 6 and 7). This difference is considered to be the result of some pore pressure dissipation. Support for this hypothesis can be drawn from the significant rate of excess pore pressure dissipation in piezometer 42 (after the end of construction to 7.25 m thickness) compared to piezometer 44 (which showed an essentially constant excess pore pressure) and the fact that piezometer 42 was much closer to the drainage boundary. Piezometer 44 indicated excess pore pressures close to the applied vertical stress at the ground surface for embankment thicknesses between 1.3 m and about 5 m. After the embankment was construction to 7.25 m thickness, the excess pore pressure remained essentially constant until the end of the monitoring period at piezometer 44. Piezometer 38 also did not indicate significant changes in the excess pore pressure during this period, but it failed to function after about 700 h. An essentially constant excess pore pressure response after failure of the embankment was also observed by Rowe et al. (1995) for the reinforced section of this test embankment. This type of response has been previously observed in soils susceptible to progressive failure (see Lo 1966; and Fisher et al. 1982*a*, 1982*b*).

Figure 8 shows that the excess pore pressure responses for piezometers 48 and 49 were very similar, although piezometer 49 indicated slightly higher excess pore pressure than piezometer 48 most of the time. Piezometers 47, 48, and 49 were placed on a vertical line beneath the slope of the embankment (see Fig. 3). The deeper piezometers reflected an increase in pore pressure in excess of that expected due to the fill directly above the piezometers. This is considered to be a result of the lateral spreading of the pore pressure from beneath the main portion of the embankment outwards reflecting the 2D nature of the excess pore pressures. An additional factor contributing to the difference in excess pore pressures at the three depths is the shorter drainage paths for the shallower piezometers resulting in more rapid dissipation of excess pore pressure. Piezometer 50, which is located beneath the toe of the embankment, showed some increase in pore pressure but, as would be expected, the level of excess pore pressure is consistently lower than that at piezometers beneath the embankment.

The reinforced embankment was raised until failure once the unreinforced embankment was at a constant thickness of 3.4 m. It is possible for pore water migration to occur under the unreinforced embankment as a result of this construction. Consequently, the pore pressure increases observed in the unreinforced section would have been influenced by the 3D effect of this construction.

Variations of parameter $\bar{B}$ (change in excess pore pressure divided by the change in vertical stress on the original ground at the centerline of the embankment = $\Delta u/\gamma\Delta H$) with time for piezometers 37, 38, and 40 (which were placed in the region close to the centerline) are presented in Fig. 9. The changes in pore pressure and vertical stress are relative to those existing at 525 h, since it was after this time that the embankment was constructed quite rapidly from 3.4 to 7.25 m (with a brief stoppage of construction at 6.25 m thickness). It is considered that the foundation soil exhibited essentially an "elastic" response up to about 3.65 m thickness, as discussed later in this paper. Piezometer 37 showed a very rapid increase of the parameter $\bar{B}$ up to about 570 h (and especially between about 560–570 h) as the embankment was raised from 5.5 to 6.25 m, and reached a maximum of 0.77 at about 595 h, after being constant at about 0.75 for a period of about 20 h. Piezometers 38 and 40 also showed very rapid increases of $\bar{B}$ values until 595 h, indicating maximums of 0.83 and 0.75, respectively, followed by a gradual decrease in these values.

Fig. 8. Excess pore pressure variation with time for piezometers 47, 48, 49, and 50.

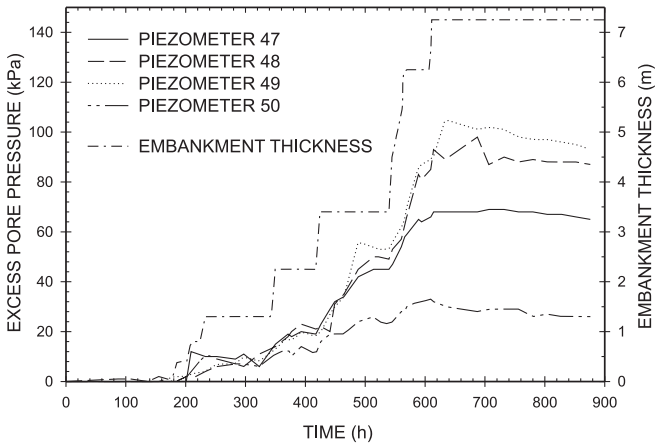

Fig. 9. Variation of parameter $\bar{B}$ with time for piezometers 37, 38, and 40 (based on time equal to 525 h).

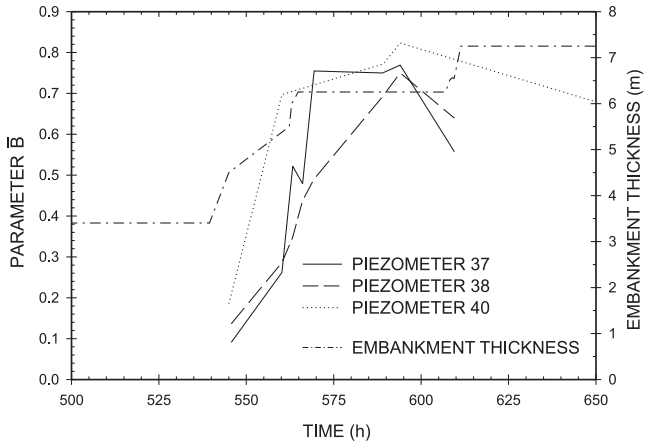

Fig. 10. Variation of horizontal displacement with depth for inclinometer 50I.

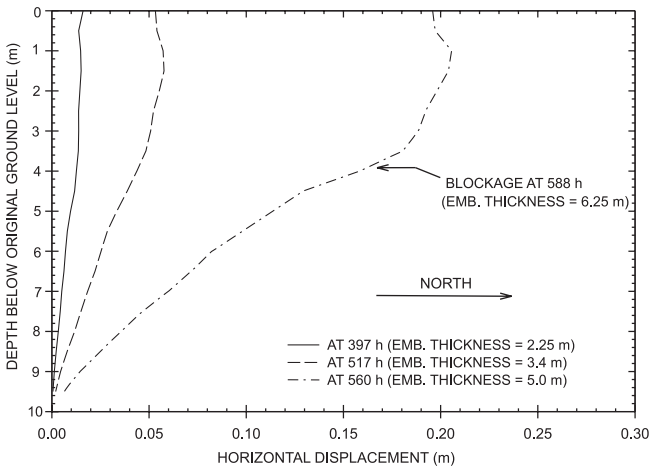

Fig. 11. Variation of horizontal displacement with depth for inclinometer 51I.

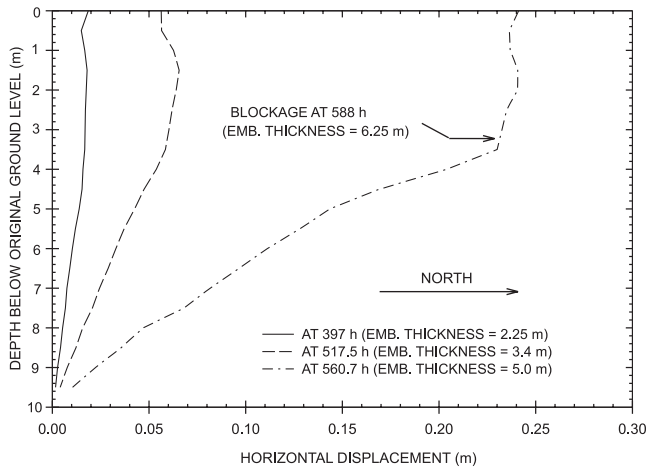

Horizontal displacement

Three inclinometer casings were installed in the region where large horizontal displacements were expected to occur (see Fig. 3). The variations of horizontal displacement with depth obtained by monitoring inclinometers 50, 51, and 52 at different embankment thicknesses are presented in Figs. 10, 11, and 12, respectively. All three inclinometers indicated very similar, small (less than 0.06 m), horizontal displacement responses up to 3.4 m thickness. This reflects an essentially elastic response of the foundation soil up to at least 3.4 m fill thickness.

The maximum lateral displacements at 50, 51, and 52 inclinometers, when the reinforced portion of the embankment failed, were of the order of 0.06 m. At this time, the top elevation of the unreinforced embankment was 3.4 m, and cracking appeared in the western portion of the embankment. Based on the lateral displacement data and observation of the cracking, it can be inferred that the behaviour of the unreinforced portion of the embankment was influenced by the failure of the reinforced embankment.

A rapid increase in the horizontal displacement, to a maximum of about 0.24 m, was observed when the embankment thickness was raised to 5 m. Being placed on the slope of the embankment, inclinometers 50 and 51 indicated larger horizontal displacements than inclinometer 52, which was placed on the crest. As a result of the relatively large movements, the inclinometers became blocked between a fill thickness of 5 and 6 m and could no longer be monitored. A probe was used to establish the depth to the inclinometer blockage at a later stage and, by inference, the depth to the failure zone shown on Figs. 10–12.

Marche and Chapuis (1974) suggested that lateral displacements could be considered a good indicator of the development of failure conditions in the foundation. However, Tavenas et al. (1979) have suggested that the development of large lateral displacements is related to the passage of the clay from an overconsolidated to a normally consolidated state (i.e., a phenomenon not directly related to the factor of safety of the foundation). For the Sackville test embankment reported here, comparison of the horizontal displacement profiles at different embankment thicknesses (e.g., for inclinometer 50 in Fig. 10) indicates a gradual initiation of a failure zone at a depth of about 3.5–4 m below the original ground surface. This observation is further confirmed by the measurements of the depth to blockage performed at later stages of construction. The horizontal displacement profiles

Fig. 12. Variation of horizontal displacement with depth for inclinometer 52I.

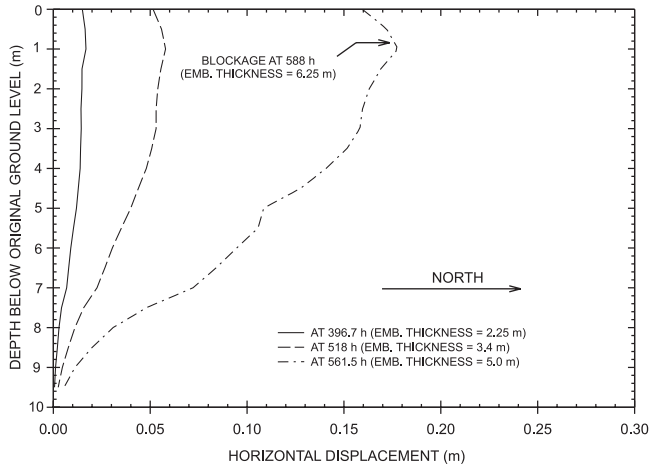

Fig. 13. Variation of settlement with time for settlement plates 32S, 33S, 34S, and 35S.

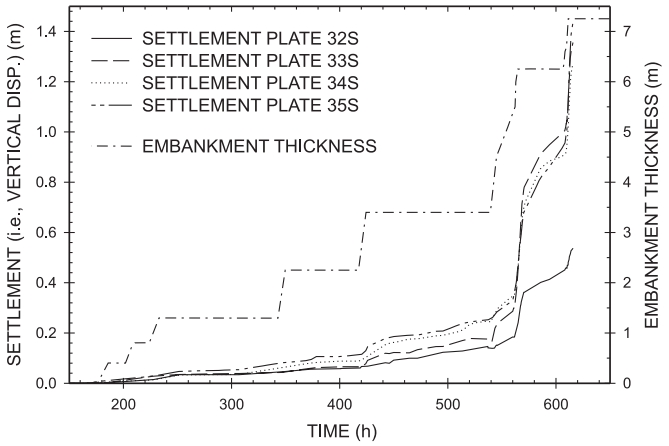

Fig. 14. Variation of settlement with time for augers 36A, 37A, and 38A.

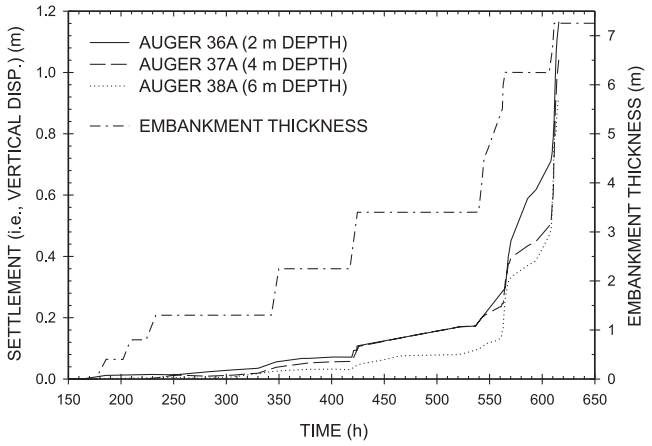

Fig. 15. Variation of vertical displacement with time for heave plates 28H, 29H, 30H, and 31H.

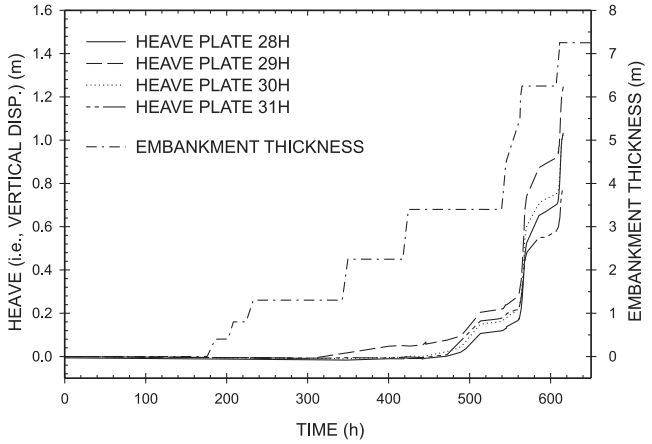

for inclinometer 51 (shown in Fig. 11) indicate the initiation of a failure zone at a depth of about 3.5 m more clearly than that for inclinometer 50. Based on the shape of the deformed profile at a fill thickness of 5 m and the location of the blockage at 6.25 m fill thickness, it would appear that the failure at the location of inclinometer 52 passed through the foundation at a depth of about 1 m, although there was significant movement in the zone to 3 m depth in the foundation and here the failure zone could be as deep as 3 m.

Settlement

The variation of settlement with time for plates 32S, 33S, 34S, and 35S is presented in Fig. 13. A similar plot for the augers 36A, 37A, and 38A is shown in Fig. 14. It can be observed that the settlements at the ground surface monitoring points (i.e., settlement plates 32S, 33S, 34S, and 35S) were relatively small (less than 0.2 m) until the embankment was constructed up to 3.4 m thickness. The plots indicate that there was a gradual increase in settlement between stages of construction when there was no addition of fill (i.e., at fill thicknesses 1.3, 2.25, and 3.4 m). The settlements were less than 0.25 m until the embankment was increased above 3.4 m. The nearby reinforced embankment section was loaded to failure, increasing its thickness from 3.4 to 9.5 m, while the unreinforced embankment thickness remained constant at 3.4 m between 425 and 540 h. The increase in settlement observed at this 3.4 m constant thickness is primarily due to the construction of the adjacent reinforced embankment to failure.

Being located beneath the slope of the embankment, the settlement at plate 32S did not increase as much as it did at the other monitoring points. The settlement at plates 33S, 34S, and 35S increased rapidly with the increase in fill thickness beyond 3.4 m during stage 4 construction (see Fig. 13). A rapid increase in settlement was evident after about 560 h (i.e., for fill thicknesses greater than 5.5 m). When the fill thickness was raised to about 6.25 m, the settlement increased up to 0.9 m. Failure of the embankment appears to have commenced at an embankment thickness of about 5.5 m, as evidenced by the blockage of the inclinometer casings between a thickness of 5 and 6 m and by the very rapid increase in settlement when the fill thickness was raised above 5.5 m (see Figs. 13 and 14). However, the failure was not dramatic and additional fill could be placed. At a fill thickness of 7.25 m, a settlement of more than 1.4 m was recorded at plate 35S. Settlements were also large at monitoring points 33S (max. settlement = 1.37 m) and 34S (max. settlement = 1.3 m).

Fig. 16. Variation of vertical displacement with time for heave plates 47H, 48H, and 49H and settlement plates 45S and 46S.

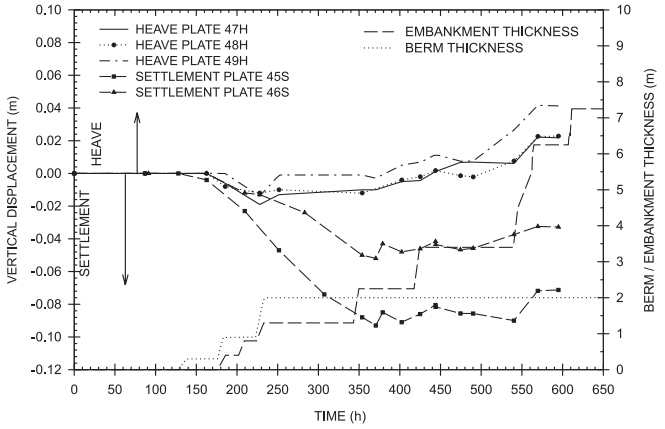

Fig. 17. Variation of settlement with embankment thickness for settlement plates 32S, 33S, 34S, and 35S.

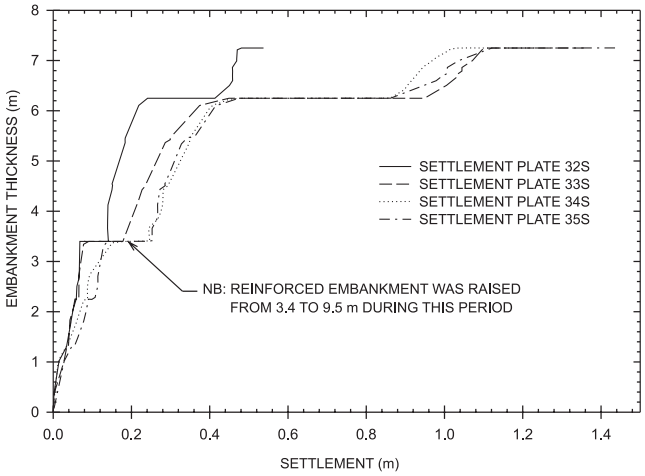

The settlement of the augers exhibited a response similar to the settlement plate points. The settlement of augers 36A and 37A was almost the same until about 550 h. A marked increase in the settlement of auger 36A compared to the other augers is observed after 565 h indicating a more rapid deformation of the upper 2 m of the foundation soil (see Fig. 14). The final movement readings were 1.17, 1.04, and 0.93 m for augers 36A, 37A, and 38A, respectively. A comparison of Figs. 13 and 14 shows that the settlement of plate 35S (which is closest to auger 36A, placed at a depth of 2 m) was 1.44 m compared with the corresponding "settlement" of 1.17 m at auger 36A. Although the augers are primarily intended to measure vertical deformations, the development of sliding (and the consequent lateral movement) will also be reflected in the "settlement" readings (since the top of the rod connected to the auger was the point actually monitored by an automated electromagnetic distance measuring apparatus). An examination of all of the available data would suggest that a significant component of the "deep settlements" noted above for augers 37A and 38A may in fact be a reflection of the lateral movement that occurred above this depth.

Fig. 18. Variation of vertical displacement with embankment thickness for heave plates 28H, 29H, 30H, and 31H.

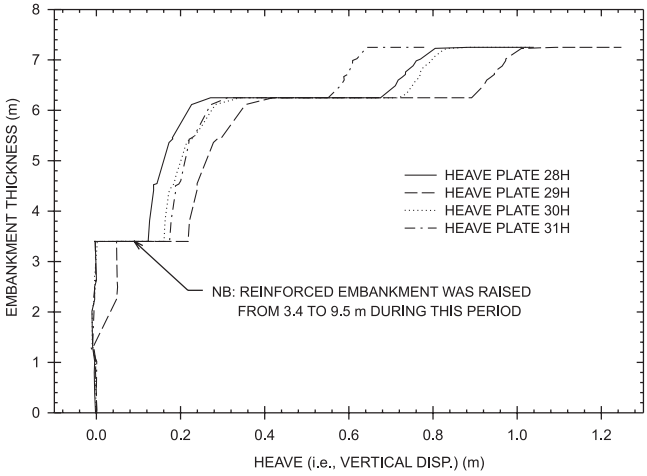

Fig. 19. Variation of net embankment height with thickness for settlement plates 33S, 34S, and 35S.

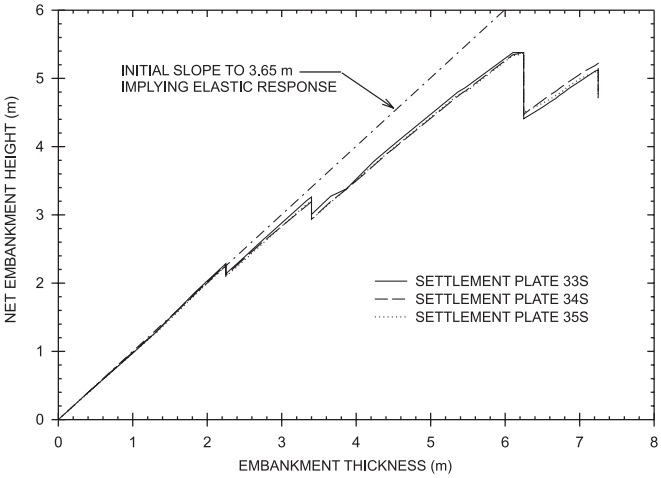

Heave

The settlements were accompanied by heave observed in the region close to the toe (see Fig. 15). Heave plates were installed at selected points in this region as detailed previously (see Figs. 1 and 3). The displacement of each heave plate was measured by monitoring the movement of the top of the 0.5 m pipe fixed perpendicular to the plate. Figure 15 indicates that the vertical displacement (i.e., heave) was small, less than 0.1 m, up to about 490 h (corresponding to an embankment thickness of 3.4 m). A small increase in heave is also observed between the stages of construction, similar to settlement observations. There was an increase in the rate of heaving at these plates between 490 and 512 h while the embankment thickness remained constant at 3.4 m, apparently due to the rapid construction of the reinforced section from 5.7 m until failure at 8.2 m thickness. However, the increased rate of heaving lasted for only about 22 h (i.e., between 490 and 512 h) and its contribution to the overall heave at these heave plate locations was small (estimated to be less than 0.09 m). This was followed by a smaller rate of increase which persisted until the embankment was raised above 3.4 m thickness.

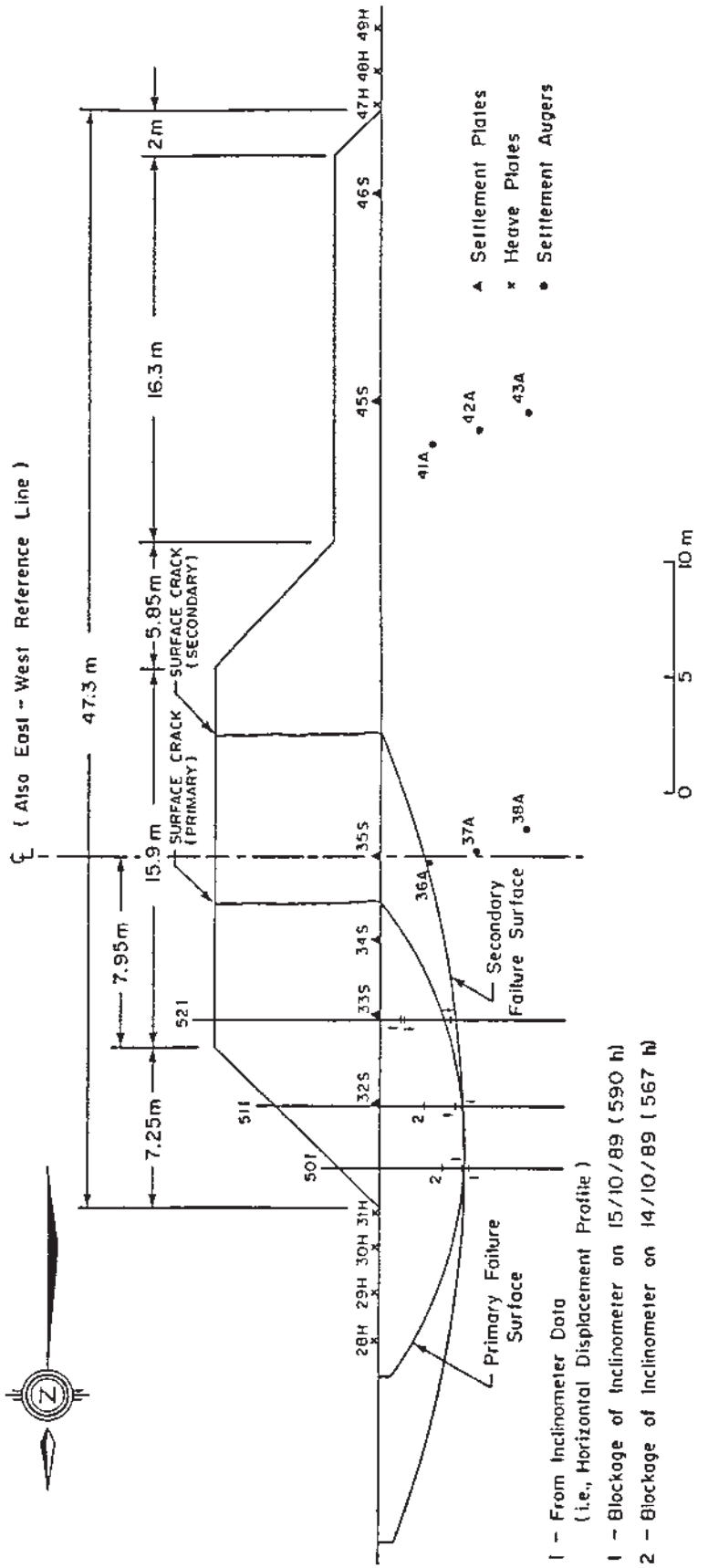

Fig. 20. Inferred failure surfaces.

A moderate increase in heave (up to a maximum of 0.28 m at heave plate 29H) was observed during the early portion of stage 4 construction (up to about 561 h). The heave increased very rapidly (by about 0.37 m at heave plate 29H) during the time 561–568 h, which reflects the increase of embankment thickness from 5.5 to 6.25 m. Settlement and inclinometer data suggested the initiation of failure during this period as previously discussed. Another period of very rapid increase in heave, by about 0.33 m at heave plate 29H, was observed during 608–616 h when the fill thickness was increased from 6.45 to 7.25 m.

Displacements on the berm side of the embankment

The settlement on the berm side of the embankment was comparatively small (< 0.1 m) as is evident from the settlement plots for settlement plates 45S and 46S (Fig. 16). Settlement plate 46S, placed close to the toe of the berm, showed significantly lower settlement than settlement plate 45S, which was placed near the middle of the berm. Both settlement plates showed an increase in settlement with time (up to about 350 h) while the main embankment thickness was less than the berm thickness. Subsequent increases in the main embankment thickness slowed and then reversed the settlement trends beneath the berm. The apparent decrease in settlement is attributed to incremental heave induced by the construction of the main embankment.

The vertical displacement observed in the heave plates placed on the southern side of the embankment was small (see Fig. 16). The largest heave observed was about 0.04 m at heave plate 49H.

Unreinforced embankment failure

The variation of settlement at plates 32S, 33S, 34S, and 35S with embankment thickness is shown in Fig. 17. A reasonably linear relationship is indicated during the early stages of construction up to about 3.4 m; apparently due to the "elastic" behaviour of the foundation soil. This is consistent with the findings of Tavenas et al. (1974) who demonstrated that foundations behave elastically up to a critical height approximately equal to 50% of the failure height. When the embankment was increased from 3.4 to 5.4 m there was initially a thickness–settlement response similar to that in the initial phase of loading. From 5.4 m there was an increased rate of settlement that became even more evident at a thickness of 6.1 m. The embankment continued to settle very rapidly even when the construction was stopped for a brief period at 6.25 m thickness. The failure appeared to be of a progressive nature, and was influenced to some degree by the disturbance caused by the failure of the reinforced embankment. To confirm progressive failure, more fill was added and the movement of the embankment was closely monitored. Construction was stopped when very rapid movements were observed at a thickness of 7.25 m.

The variation of vertical displacement with embankment thickness at the heave plates placed north of the toe is shown in Fig. 18. The heave was generally small compared to the settlement for fill thicknesses up to 3.4 m. The heave responses indicate that nonlinear behaviour started to occur between 3.4 and 4.5 m thickness, well before the 5.4 m thickness indicated by the settlement responses. The gradual flattening of the settlement and heave responses as the fill thickness approached 6.25 m suggests that the failure thickness of the embankment was close to 6.25 m. However, a definite failure thickness cannot be interpreted from these figures.

A linear relationship for the variation of net embankment height with embankment thickness up to about 3.65 m thickness is evident in Fig. 19. The net embankment height is defined as the elevation of the crest of the embankment with reference to the maximum elevation of the ground near the toe. The net embankment height increased linearly with embankment thickness during the first three stages of construction and up to about 3.65 m thickness during stage 4 construction (as evident from this figure), apparently due to the elastic behaviour of the foundation soil. A gradual change in the slope of the net height versus thickness response after 3.65 m was evident, indicating a nonlinear response beyond this thickness. A rapid flattening of the variation of net embankment height with thickness is observed at an embankment thickness of 6.1 m (i.e., at about 5.4 m net height) indicating the onset of failure of the embankment. This thickness corresponds to a time of 565 h (see Fig. 4). At this time, very rapid increases in settlement (see Figs. 13 and 14) as well as heave (see Fig. 15) were observed, as reported earlier. The net embankment height remained constant at about 5.4 m until the embankment was raised to 6.25 m thickness, indicating a plastic (or viscoplastic) type of failure of the embankment. The net height then decreased significantly (to about 4.5 m) at a fill thickness of 6.25 m even though there was no addition of fill between 565 and 607 h and despite the fact that there was no significant decrease in the excess pore pressures during this period.

To confirm the failure of the embankment, more fill was added starting at about 607 h. The embankment height increased gradually again, but at a lesser gradient up to a maximum of about 5.2 m. The construction was stopped at 7.25 m thickness when very rapid settlement and heave was observed, as discussed previously (see Figs. 13 and 15). The net embankment height dropped to about 4.8 m within 2 h. It was evident that the embankment had already failed and that this failure was of a viscoplastic type. It was clear that the embankment could not be constructed significantly above the net height of 5.4 m, which was first reached at a fill thickness of 6.1 m.

The failure thickness of 6.1 m indicated by this field investigation is lower than the 7.0–11.4 m range indicated by limit equilibrium analysis performed on the basis of vane test data. A limit equilibrium analysis performed on the basis of the average vane strength profile for the foundation soil (for a 6.1 m thick embankment) indicated factors of safety of about 1.59 and 2.34, respectively, for the primary and secondary failure surfaces inferred from the field investigation (see Fig. 20). Similar limit equilibrium analysis performed for the reinforced embankment predicted its failure thickness well, but did not predict a unity safety factor for the failure surfaces inferred in the field (see Rowe et al. 1995). It is noted that the plasticity index of the soil ranged between 9 and 19% (see Fig. 2) with an average of about 14%, and the corresponding Bjerrum's correction for the

vane strength will not have a significant effect on either the calculated failure thickness or the factor of safety (see Bjerrum 1973). It is thought that progressive failure, in combination with disturbance of the foundation soil when the reinforced section failed, contributed to the lower failure thickness observed in this field investigation. Thus, the data reported in this paper can be used as a test case for developing or validating 3D analysis methods and (or) models wherein the constitutive model can be truly tested for 3D conditions involving the interaction between embankment sections that are constructed under different conditions.

General comments on the performance of the instrumentation

The position monitoring devices (i.e., settlement plates, augers, and heave plates) performed very well during the entire construction and monitoring period. The electronic distance-measuring apparatus allowed quick readings and automatic recordings on a computer. The inclinometers provided useful data up to about 5 m thickness but could not be monitored afterwards due to the relatively large movements. The pneumatic piezometers functioned well and provided useful data for most of the construction period, at least up to about 6.25 m thickness. Out of the ten pneumatic piezometers functioning at the beginning of construction, seven were still functioning and appeared to be giving reasonable readings at the end of testing. The pneumatic total pressure cell also functioned well and provided useful data throughout the construction and monitoring period.

Summary and conclusions

The instrumentation and field performance of the unreinforced section of the test embankment constructed at Sackville, N.B. has been described. This embankment was instrumented with piezometers, settlement plates, augers, heave plates, inclinometers, and a total pressure cell.

The embankment behaved elastically up to a thickness of about 3.65 m. The nearby reinforced section was constructed to failure when the unreinforced section was at a constant thickness of 3.4 m. The unreinforced section was constructed rapidly from 3.4 to 6.25 m thickness. Examinations of pore pressure, heave, and settlement responses suggest that the embankment failed at a thickness of 6.1–6.25 m. The net height could not be raised above a maximum of 5.4 m (attained at a fill thickness of about 6.1 m) even though the fill thickness was eventually increased from 6.25 to 7.25 m. The failure was gradual and of a viscoplastic type and no classical-type abrupt failure was encountered during the construction of this embankment.

The failure surfaces inferred from inclinometer data and surface observations indicate that the failure was at or above 4 m depth. It is thought that a significant part of the apparent settlement of the auger at 6 m depth may be due to lateral movements that occurred above this depth.

The height to which the embankment could be constructed is substantially less than what would be expected based on a conventional 2D limit equilibrium calculation using conventional vane strength data. This, coupled with the pore pressure response, suggests that progressive failure combined with strength reduction of soil while loading the reinforced section to failure may have been significant in the performance of this embankment.

The data reported in this paper can be used for developing 3D analysis methods wherein the constitutive model can be truly tested for 3D conditions involving the interaction between embankment sections that are constructed under different conditions.

Acknowledgements

The construction and monitoring of the test embankment was funded by the Natural Science and Engineering Research Council of Canada by means of Strategic Grant STR12092. The authors also wish to acknowledge the assistance of Mr. K. White in the installation of instruments and monitoring of the embankment.

References

Asaoka, A., Noda, T., and Fernando, G.S.K. 1998. Consolidation deformation behaviour of lightly and heavily overconsolidated clay foundations. Soils and Foundations, Japanese Geotechnical Society, **38**: 75–91.

Bjerrum, L. 1973. Problem of soil mechanics and construction on soft clays. *In* Proceedings of the 8th International Conference on Soil Mechanics and Foundation Engineering, Moscow, State of the Art Report, Vol. 3, pp. 111–159.

Crawford, C.B., Fannin, R.J., and Kern, C.B. 1995. Embankment failures at Vernon, British Columbia. Canadian Geotechnical Journal, **32**: 271–284.

D'Appolonia, D.J., Lambe, T.W., and Poulos, H.G. 1971. Evaluation of pore pressures beneath an embankment. Journal of Soil Mechanics and Foundation Engineering, ASCE, **97**: 881–897.

Fernando, G.S.K. 1996. Non-linear consolidation deformation analysis of soils under embankment loading. D. Eng. thesis, Department of Civil Engineering, Nagoya University, Chikusa-ku, Japan.

Fisher, D.G., Rowe, R.K., and Lo, K.Y. 1982*a*. Prediction of second stage behaviour of the Gloucester Test Fill – Part 1: Predictions. Research Report GEOT-3-82, Faculty of Engineering Science, University of Western Ontario, London, Canada.

Fisher, D.G., Rowe, R.K., and Lo, K.Y. 1982*b*. Prediction of second stage behaviour of the Gloucester Test Fill – Part 2: Method of Analysis. Research Report GEOT-4-82, Faculty of Engineering Science, University of Western Ontario, London, Canada.

Hinchberger, S.D., and Rowe, R.K. 1998. Modelling the rate-sensitive characteristics of the Gloucester foundation soil. Canadian Geotechnical Journal, **35**: 769–789.

Hoeg, K., Andersland, O.B., and Rolfsen, E.N. 1969. Undrained behaviour of quick clay under load tests at Astrum. Géotechnique, **19**: 101–115.

Hussein, A.N., and McGown, A. 1998. The behaviour of two trial embankments at Perlis, Malaysia with different rates of construction. *In* Proceedings of the 4th International Conference on Case Histories in Geotechnical Engineering, St. Louis, Missouri, 8–12 May, *Edited by* S. Prakash. GeoResearch International Inc., Ottawa, Canada, pp. 454–457.

Indraratna, B., Balasubramaniam, A.S., and Balachandran, S. 1992. Performance of test embankment constructed to failure on soft marine clay. Journal of Geotechnical Engineering, ASCE, **118**: 12–33.

Leroueil, S., and Rowe, R.K. 2000. Embankments over soft soil and peat. *In* Geotechnical and geoenvironmental engineering handbook, Kluwer Academic Publishing, Norwell, U.S.A. pp. 463–499.

Leroueil, S., Tavenas, F., Trak, B., La Rochelle, P., and Roy, M. 1978*a*. Construction pore pressures in clay foundations under embankments. Part I: the Saint-Alban test fills. Canadian Geotechnical Journal, **15**: 54–65.

Leroueil, S., Tavenas, F., Mieussens, C., and Peignaud, M. 1978*b*. Construction pore pressures in clay foundations under embankments. Part II: generalized behaviour. Canadian Geotechnical Journal, **15**: 66–82.

Lo, K.Y. 1966. The stress-strain pore pressure relationship of normally consolidated clays. Ph.D. thesis. University of London, England.

Loganathan, N., Balasubramaniam, A.S., and Bergado, D.T. 1993. Deformation analysis of embankments. Journal of Geotechnical Engineering, ASCE, **119**: 1185–1206.

Marche, R., and Chapuis, R. 1974. Contrôle de la stabilité des remblais par la mesure des désplacements horizontaux. Canadian Geotechnical Journal, **11**: 182–201.

Ortigao, J.A.R., Werneck, M.L.G., and Lacerda, W.A. 1983. Embankment failure on clay near Rio De Janeiro. ASCE Journal of the Geotechnical Engineering Division, 109, **11**: 1460–1479.

Parry, R.H.G., and Wroth, C.P. 1981. Shear stress-strain properties of soft clay. *In* Soft clay engineering. *Edited by* E.W. Brand and R.P. Brenner, Elsevier Scientific Publishing Company. pp. 311–362.

Rampton, V. N., and Paradis, S. 1981. Quarternary geology of Amherst – Map area 21H, New Brunswick. Mineral Development Branch, Department of Natural Resources, Fredericton, New Brunswick, Map report 81–3.

Rowe, R.K., and Hinchberger, S.D. 1998. The significance of rate effects in modelling the Sackville test embankment. Canadian Geotechnical Journal, **35**: 500–516.

Rowe, R.K., Gnanendran, C.T., Landva, A.O., and Valsangkar, A.J. 1995. Construction and performance of a full-scale geotextile reinforced test embankment, Sackville, New Brunswick. Canadian Geotechnical Journal, **32**: 512–534 [Errata, **33**: 208(1996)].

Tavenas, F., and Leroueil, S. 1980. The behaviour of embankments on clay foundations. Canadian Geotechnical Journal, **17**: 236–260.

Tavenas, F., Chapeau, C., La Rochelle, P., and Roy, M. 1974. Immediate settlements of three test embankments on Champlain clay. Canadian Geotechnical Journal, **11**: 109–141.

Tavenas, F., Mieussens, C., and Bourges, F. 1979. Lateral displacements in clay foundations under embankments. Canadian Geotechnical Journal, **16**: 532–550.